Information Sciences 232 (2013) 88–103

Contents lists available at SciVerse ScienceDirect

Information Sciences

journal homepage: www.elsevier.com/locate/ins

A new distributed cooperative MIMO scheme for mobile ad hoc networks

Renato M. de Moraes [a,*], Hyunchul Kim [b], Hamid R. Sadjadpour [b], J.J. Garcia-Luna-Aceves [b]

[a] Department of Electrical Engineering, University of Brasília, DF 70910-900, Brazil
[b] Department of Electrical and Computer Engineering, University of California at Santa Cruz, 1156 High Street, Santa Cruz, CA 95064, USA

ARTICLE INFO

Article history:
Received 30 December 2009
Received in revised form 24 February 2012
Accepted 28 December 2012
Available online 8 January 2013

Keywords:
Ad hoc network
Ergodic capacity
Information theory
MIMO system

ABSTRACT

In this paper, we introduce a new communication scheme based on cooperative multiple-input multiple-output (MIMO) communication for mobile ad hoc networks (MANETs) in which nodes are endowed with M antennas. According to our new approach, adjacent nodes no longer interfere with each other but rather cooperate attempting to communicate concurrently. In our scheme, during transmissions, the nodes send packets from only one of their antennas, while during reception, they use all of their antennas to receive and decode packets from multiple close nodes simultaneously. Therefore, each distributed MIMO system in this scheme consists of multiple transmitting nodes acting as a single-array of multiple antennas. We derive upper and lower bounds on the receiver node ergodic capacity in the network where the wireless channel is modeled with both large and small-scale fluctuations. These bounds are compared with Monte-Carlo simulation of point-to-point and cooperative MIMO communications in MANETs. We demonstrate that the capacity of MANETs with multiple antennas is improved using cooperation compared to non-cooperative schemes, i.e., point-to-point MIMO communication. In addition, under the above communication model, we demonstrate that the lower and upper bounds of the ergodic capacity grows linearly with the number of receiving antennas M.

1. Introduction

The studies for capacity of MIMO systems concentrated on the communication between two nodes, i.e., point-to-point (or one-to-one) communication and was first investigated in [1–3]. The work by Jovičić et al. [4] studies the capacity of wireless ad hoc networks by assuming that the entire network is a single MIMO system in which some nodes are part of the transmitter and the remaining nodes in the network are part of the receiver, and where all the nodes have only one antenna. In a similar strategy, Luan and Gao [5] proposed a MIMO strategy for ad hoc networks considering clusters of transmitters and receivers to act as an array of multiple transmitter and receiver antennas, respectively, and showed that the bit error rate performance for their approach outperforms the point-to-point case. These results are optimistic by assuming all the receiving nodes in the network are capable of cooperating with each other to decode the data. Furthermore, Chen and Gans [6] and Blum [7] addressed the problem of capacity for MIMO ad hoc networks assuming fading for the wireless channel. However, both works only consider small-scale fluctuations of the fading channels. Accordingly, Chen and Gans [6] showed that the node capacity of a MIMO ad hoc network goes to zero as the total number of nodes n increases, because all the interfering nodes have the same average power at the receiver node regardless of their distance from the receiving node.

* Corresponding author. Tel.: +55 (61) 31075583; fax: +55 (61) 31075590.
E-mail addresses: renatomdm@unb.br (R.M. de Moraes), hyunchul@soe.ucsc.edu (H. Kim), hamid@soe.ucsc.edu (H.R. Sadjadpour), jj@soe.ucsc.edu (J.J. Garcia-Luna-Aceves).

0020-0255/$ - see front matter © 2013 Elsevier Inc. All rights reserved.
http://dx.doi.org/10.1016/j.ins.2012.12.042

Other previous works [8–10] have proposed cooperation strategies with MIMO techniques for static wireless ad hoc networks investigating the throughput scaling laws in which the objective is to overcome the Gupta and Kumar's results of vanishing capacity according to $\Theta\left(\frac{1}{\sqrt{n}}\right)$ [11].[1] In all of them, they arrive at the conclusion that the capacity is a function of n^{δ}, in which the power law exponent (δ) varies according to the transmission scheme employed.

On the other hand, more recent papers on MIMO ad hoc networks have focused on the problem of exploiting diversity of a single pair of nodes employing point-to-point communication. In [12], Jindal et al. showed that even a single-input multiple-output (SIMO) transmission approach in ad hoc networks can attain capacity growing linearly with the number of the receiving antennas as long as simultaneous interference cancelation is employed to allow the increase of received power of the desired signal. Zaharov and Kettani [13] investigated the behavior of MIMO ad hoc networks in the presence of interference and proposed an adaptive beamforming scheme to improve the point-to-point communication performance. In [14], Elbatt proposed a unified framework considering scheduling, multiplexing and diversity trade-off in MIMO ad hoc networks to address the point-to-point communication approaches.

Referring to distributed collaboration strategies, Qu et al. [15] proposed a cooperative MIMO scheme for ad hoc networks in which a node dynamically chooses its destination nodes having multiple antennas and adaptively allocates the power and adjusts the constellation size trying to optimize these parameters to improve system performance. However, they do not assume other source nodes concurrently transmitting nor consider interference as we may expect in ad hoc networks. In [16], a cooperative MIMO approach was proposed to opportunistically schedule simultaneous transmission maximizing data rate in ad hoc networks. Nevertheless, in order to efficiently coordinate the concurrent transmissions, the scheme relied in part on a centralized algorithm which is not appropriate for ad hoc networks because they are infrastructureless systems by definition.

In most of all previous work, the main effort to improve capacity was to overcome the destructive interference effect due to bandwidth sharing in the common communication channel. In [17,18], it was introduced a new cooperation scheme based on collaboration among nodes which allows simultaneous multipacket transmission and reception with multi-copy relaying aiming delivery delay reduction in MANETs. Inspired by these works [17,18], this paper extend such studies to MANETs employing a distributed MIMO communication in which large-scale fluctuations of the channel is included. More specifically, the present paper proposes a strategy for communication among nodes in wireless mobile ad hoc networks based on cooperative MIMO communication [17,18], which permits multipacket transmission and reception. It also allows multi-copy transmission of the same packet in order to reduce delivery delay. In this new paradigm, multiple nodes that are close to each other attempt to communicate concurrently. Nodes transmit and receive simultaneously using different portions of the available spectrum, which characterizes a frequency division multiple access (FDMA)/MIMO approach. During transmission, the node sends packets from only one of its antennas, while during reception, it uses all of its antennas to receive and decode packets from multiple nodes simultaneously. Thus, each distributed MIMO system in this scheme consists of multiple transmitting nodes acting as a single-array of multiple antennas, and a single receiver node with multiple antennas in a cell. Consequently, the nodes collaborate with each other by relaying one another packets, which reduces delivery delay [19]. This approach does not require any coordination among receiving nodes for decoding the received packets.

We present lower and upper bounds on the channel capacity of MIMO MANETs when the wireless channel is modeled with both large and small-scale fluctuations. We show that receiver node ergodic capacity does not depend on the total number of nodes n; however, it is a function of such other network parameters as the number of receiving antennas, cell area, average node density, noise spectral density, and the path loss parameter. It is also shown that the total bandwidth required is finite for the proposed FDMA/MIMO system.

This paper is organized as follows. Section 2 presents the network and communication models detailing the distributed MIMO cooperative scheme proposed. Section 3 reports the capacity analysis computing upper and lower bounds. Section 4 shows the numerical and simulation results comparing the obtained bounds with Monte-Carlo simulations. We conclude the paper in Section 5.

2. Model

2.1. Network model

Consistent with prior works [11,19–23], we make the following assumptions: (a) there is a total of n mobile nodes in the network, (b) the channel is time-slotted to simplify the analysis, (c) the power chosen by a node to transmit to another node is constant and equal to P, and (d) each node transmits data to another node using a half-duplex[2] wireless link frequency bandwidth of ΔW.

Furthermore, we assume that the total area of the network grows linearly with n. Accordingly, the modeling problem we address is that of a MANET in which n mobile nodes move in the total network area. The network is divided in cells. To simplify our analysis, the cells have square shapes, each with area equal to a_{cell} that does not depend on n. We assume that communication occurs only among those nodes that are close enough, i.e., nodes that are in the same cell, so that interference

[1] According to Knuth's notation, $f(n) = \Theta(g(n))$ means there are positive constants c_1, c_2, and k integer, such that $0 \leqslant c_1 g(n) \leqslant f(n) \leqslant c_2 g(n)\ \forall n \geqslant k$.

[2] Half-duplex means that a node cannot transmit and receive data simultaneously through the same frequency bandwidth ΔW.

caused by nodes farther away is low, allowing reliable communication. Our packet-delivery scheme [19] resembles the one introduced by Grossglauser and Tse [21], and is such that a source relays a packet to one or more one-time relays that move throughout the network and deliver a single copy of the packet to the destination.

The position of node i at time t is indicated by $X_i(t)$. Nodes are assumed to move according to the *uniform mobility model* [24]. This model satisfies the following properties [24]: (a) the position of the nodes are independent of each other at any time t; (b) the steady-state distribution of the mobile nodes is uniform; (c) and the direction of the node movement is uniformly distributed in $[0, 2\pi)$, conditional on the position of the node.

Therefore, with the uniform mobility model, the average node density ρ and the total network area $A_T(n)$ are related by the following definition $A_T(n) := \frac{n}{\rho}$. Accordingly, the total number of cells in the network (μ) is given by

$$\mu = \frac{A_T(n)}{a_{cell}} = \frac{n}{\rho a_{cell}}. \tag{1}$$

Each node is assumed to know its own position (but not the position of any other node) by utilizing a GPS circuit [25] or some other technique, and to store a geographical map of the cells in the network with the associated frequencies as described subsequently. The GPS receiver is also assumed to provide an accurate common time reference to keep all nodes synchronized.

We use two types of channels. *Control channels* are used by nodes to obtain such information as the identities of strong interference sources, the data packets expected by destinations (which ensures the delivery of only one copy of each packet [19]), and the channel state information (CSI) (by means of training sequences). The detailed description of the control channel is beyond the scope of this paper but is provided in [17,18]. *Data channels* are used to transmit data taking advantage of FDMA/MIMO.

Each node simultaneously transmits and receives data during a communication time period, through non-overlapping frequency bands (channels), because each data link is half-duplex. This time period of communication is called a *communication session* or simply *session*. Furthermore, each session is divided into two parts. A neighbor discovery protocol is used by nodes during the first part to obtain their neighbors information (e.g., node identifier (ID)), and the transmission of data is performed during the second part. Each node has a unique ID that does not change with time. In addition, each node as a source picks an arbitrary destination to send packets and, for the purpose of our analysis, this source–destination association does not change with time.

As illustrated in Fig. 1, there are nine different cell numbers. Therefore, many cells use the same number, however they are placed regularly far apart from each other to reduce interference. Consequently, the frequency division assignment is such that each set of cells numbered from 1 to 9 employs different frequency channels, as explained in Section 2.2. Accordingly, for the cell configuration given, nodes i and j in cell 5 at the center of Fig. 1 use different frequency channels to communicate with each other such that, for any other node k located in another cell numbered as 5 and using the same frequency channels, it is true that $|X_k(t) - X_j(t)| \geqslant (1 + \Delta)|X_s(t) - X_j(t)|$, where $\Delta > 0$, so that X_k is at a distance greater than $|X_s(t) - X_j(t)|$ to node j. This is called the *protocol model* and fulfills the condition for successful communication stated by Gupta and Kumar [11]. In other words, sets of distinct frequency channels will be associated to nodes in the same cell willing to communicate and reused in other cells placed sufficient far away such that a pair of node i and j located in the same cell will be closer to each other than any other node k employing the same set of channels as i and j, i.e., k will be located in another cell distant enough in order to satisfy the *protocol model*.

Now, consider that at most $\mathcal{A}$ nodes in any cell are allowed to have a non-overlapping frequency channel for communication. We now show that the fraction of cells having more than $\mathcal{A}$ nodes can be bounded by a small constant when n is large.

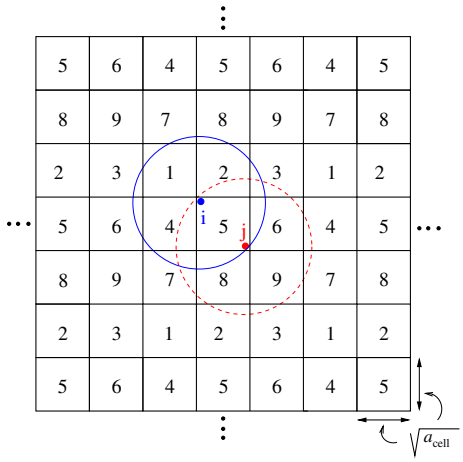

Fig. 1. Cells numbering in the network with a_{cell} as the cell area.

By applying random occupancy theory [26], considering the uniform mobility model, the fraction of cells containing $S = s$ nodes is obtained by

$$\mathbb{P}\{S = s\} = \binom{n}{s}\left(\frac{1}{\mu}\right)^{s}\left(1-\frac{1}{\mu}\right)^{n-s} = \binom{n}{s}\left(\frac{\rho\, a_{cell}}{n}\right)^{s}\left(1-\frac{\rho\, a_{cell}}{n}\right)^{n-s}. \tag{2}$$

Given that $\binom{n}{s} \approx \frac{n^s}{s!}$ for $n >> s$, and using the limit $\left(1-\frac{1}{x}\right)^{x} \to e^{-1}$ as $x \to \infty$, we have

$$\lim_{n\to\infty}\mathbb{P}\{S = s\} = \frac{1}{s!}(\rho\, a_{cell})^{s} e^{-\rho\, a_{cell}}. \tag{3}$$

The fraction of cells having more than $\mathcal{A}$ nodes is obtained by

$$\lim_{n\to\infty}\mathbb{P}\{S > \mathcal{A}\} = \lim_{n\to\infty}\sum_{s=\mathcal{A}+1}^{n}\mathbb{P}\{S = s\} = \sum_{s=\mathcal{A}+1}^{\infty}\frac{1}{s!}(\rho\, a_{cell})^{s} e^{-\rho\, a_{cell}} = 1 - \frac{\Gamma(\mathcal{A}+1, \rho a_{cell})}{\Gamma(\mathcal{A}+1)}, \tag{4}$$

where $\Gamma(m+1) = m!$, and $\Gamma(m,x) = \int_x^{\infty} y^{m-1}e^{-y}dy$, is the incomplete Gamma function. For example, $\lim_{n\to\infty}\mathbb{P}\{S > 8\} = 0.0038$ for $\rho a_{cell} = 3$. Therefore, the fraction of cells having more than $\mathcal{A}$ nodes can be designed to be very small. Obviously, if a cell contains more than $\mathcal{A}$ nodes, only $\mathcal{A}$ nodes are allowed to participate in each communication session. The limitation on the number of nodes allowed to communicate in each cell is due to practical considerations associated with MIMO systems (e.g., hardware complexity, maximum number of receive antennas, power consumption constraint, cost, etc.).

2.2. Bandwidth allocation

With cooperative MIMO communication, many nodes transmit concurrently to many other nodes that are close enough, and all such transmissions are decoded. Hence, a node may concurrently send to and receive from multiple nodes. We present an example of how cooperative MIMO communication can be implemented with a hybrid scheme based on FDMA and MIMO that supports concurrent communications. Together with the cell arrangement given in Fig. 1, this approach reduces the effect of interference at the receivers compared to non-cooperative MIMO schemes that do not use our cell planning, since here the concurrent interferers will be located on other cells far away.

Let ξ_i denote the set of non-overlapping data frequency bands (channels) used in cell i. Accordingly, the data channels are ordered and grouped as follows: $\xi_1 = \{W_1^{(1)}, \ldots, W_{\mathcal{A}}^{(1)}\}, \xi_2 = \{W_{\mathcal{A}+1}^{(2)}, \ldots, W_{2\mathcal{A}}^{(2)}\}, \ldots, \xi_9 = \{W_{8\mathcal{A}+1}^{(9)}, \ldots, W_{9\mathcal{A}}^{(9)}\}$, in which $W_j^{(i)}$ stands for the jth bandwidth in cell i. In this way, any set of nine cells, numbered from 1 to 9 according to Fig. 1, has a non-overlapping set of frequency bands.

As mentioned earlier, the signaling in the control channel provides each node in cell i knowledge of who the other nodes in the same cell are. Each node uses this information to choose a data channel to receive data in the following order based on its own ID and the IDs of its neighbors.

- The node with the highest ID in cell i is associated (for reception) with the data channel ΔW centered at $W_{(i-1)\mathcal{A}+1}^{(i)}$ in ξ_i.
- The node with the second highest ID in cell i is associated (for reception) with the data channel ΔW centered at $W_{(i-1)\mathcal{A}+2}^{(i)}$ in ξ_i, and this continues for all nodes in cell i.

The data channels not utilized become idle in cell i. This happens in those cells where the number of nodes is smaller than $\mathcal{A}$. Accordingly, the total bandwidth required for the entire network is $\Delta W_{total} = 9\mathcal{A}\Delta W$. Because ΔW and $\mathcal{A}$ are finite, the total bandwidth necessary for the FDMA/MIMO ad hoc network is also finite.

2.3. Cooperative MIMO communication

At time t, a cell has S nodes, such that the data communication is S-to-S (see Fig. 2), where S is a random variable due to the mobility of the nodes. Each node transmits through a single antenna (employing FDMA) the same or different data packets to the other $S-1$ nodes in the same cell, using $S-1$ distinct data channels (downlink), while it simultaneously receives (through many antennas) up to $S-1$ different data packets from the other $S-1$ nodes through its assigned data channel (uplink). Hence, every node can concurrently transmit (receive) to (from) all other nodes in the same cell. Thus, multi-copies of the same packet can be simultaneously relayed to attain delivery delay reduction as shown in [19].

Consequently, as Fig. 3 illustrates, the data packet forwarding consists of two phases [19]: The packet is transmitted from the source to possibly several relay nodes during *Phase 1* (i.e., multiple copies can be forwarded), and it is delivered later to its destination by only one of the relay nodes during *Phase 2*. Both phases occur concurrently, but *Phase 2* has priority in all communications. These multiple one-time relays for the same packet provide better delay performance since the copies of the same packet follow different random routes, looking for the destination, reducing delay exponentially [19].

2.4. Communication model

Without loss of generality (wolog), let the cell where node j is currently located be denoted as cell 0. Also, assume that the other cells (employing the same set of frequencies as cell 0) are numbered from $i = 1$ to ∞. P is the transmit power chosen by

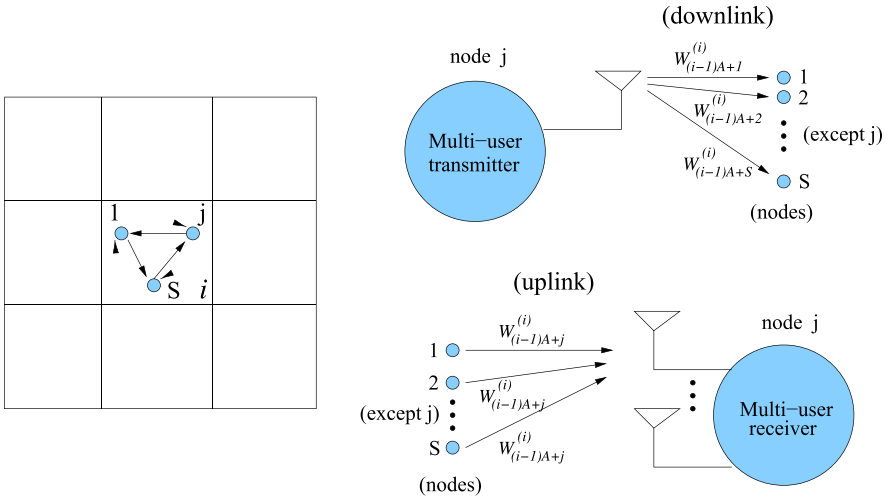

Fig. 2. FDMA/MIMO downlink and uplink description for data channels in a cell *i*. Communication is *S*-to-*S* (i.e., many-to-many).

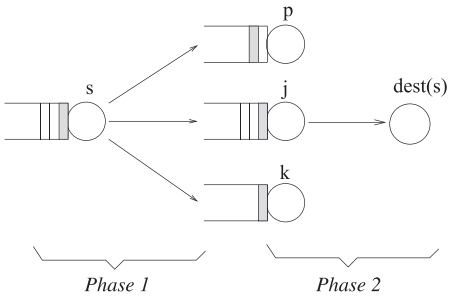

Fig. 3. Relaying scheme for a packet from node *s*: three copies of this packet are simultaneously relayed at *Phase 1* to nodes *p*, *j*, and *k*. *Node j* is the first to find the destination node dest (*s*), and delivers the packet at *Phase 2*.

node *s* to transmit to node *j*. The distance between a transmitting node *s* (located at cell *i*) and the receiver *j* is denoted as $r_{s,j}(i)$. Assuming **no fading**, the received signal power at node *j* from node *s* is [3]

$$P_{s,j}(i) = \frac{P}{\left(1 + r_{s,j}(i)\right)^{\alpha}}, \tag{5}$$

where α is the path loss parameter and assumed to be greater than or equal to 2.

In (5), $r_{s,j}(i)$ is not a function of receive antennas, i.e., *m*. The reason is that the distances between the transmitting node *s* and all *M* antennas of the receiver *j* are practically considered to be equal.

In our analysis, we consider that CSI is only known at the receiver side. Furthermore, in every cell, each MIMO system consists of multiple transmitting nodes and a single receiver node (with *M* receiving antennas), as shown in Fig. 2(uplink).

We use boldface capital letters to represent matrices and boldface lower case letters to denote vectors. In addition, the following standard notation will be used: $\prime$ for vector transpose, † for conjugate transpose of a matrix (or vector), $*$ for conjugate of a scalar, $tr(\cdot)$ for trace, $\det(\cdot)$ for determinant of a matrix and $diag(\cdots)$ for a diagonal matrix. $E_T\{\cdot\}$ denotes the expectation with respect to the random variable *T*.

The received signal vector (from cell *i*) for one receiver node *j* is defined as $\mathbf{y}_j(i) = [y_{1,j}(i), y_{2,j}(i), \ldots, y_{M,j}(i)]\prime$. The transmission vector from cell *i* is $\mathbf{x}(i) = [x_1(i), x_2(i), \ldots, x_{L_i}(i)]\prime$, where $L_i = \min(\mathcal{A}, S_i) - 1$ is the number of nodes in cell *i* allowed to transmit in the same frequency, since $\mathcal{A}$ nodes at most are permitted to transmit in each cell minus the receiver and S_i is the random variable for the number of nodes in cell *i*. We assume that the nodes in cell *i* are transmitting in the same frequency band that node *j* is using to receive data. Furthermore, transmit nodes in cell *i* use only one antenna while receiving nodes utilize all their *M* antennas for communication. Thus, the total transmitted power for a channel in the cell is L_iP. The received signal from a cell *i* for a node *j* is defined as $\mathbf{y}_j(i) = \mathbf{H}_j(i)\mathbf{x}(i) + \mathbf{z}_j$, where $\mathbf{z}_j = [z_{1,j}, z_{2,j}, \ldots, z_{M,j}]\prime$ is a zero-mean complex

[3] This path loss channel model obeys the law of conservation of energy which ensures that the received power is never greater than the transmitted power [4,27,28], as opposed to the more common approach of $1/r^{\alpha}_{s,j}(i)$ [11,19,21–23].

additive white Gaussian noise (AWGN) vector. We assume that $E[\mathbf{z}_j\mathbf{z}_j^\dagger] = \sigma_{\mathbf{z}}^2\mathbf{I}_M$, where $\mathbf{I}_M$ is the $M \times M$ identity matrix and $\sigma_{\mathbf{z}}^2$ is the noise variance. $\mathbf{H}_j(i)$ is the $M \times L_i$ channel matrix from cell i to node j with its elements defined as [4]

$$h_{ms,j}(i) := (\mathbf{H}_j(i))_{ms} = \frac{\phi_{ms,j}(i)}{(1 + r_{s,j}(i))^{\alpha}}, \tag{6}$$

where $1 \leqslant m \leqslant M,\ 1 \leqslant s \leqslant L_i$. Note that this channel modeling considers both the fading and distance effects. The fading coefficient $\phi_{ms,j}(i)$ is zero-mean, Gaussian, with independent real and imaginary parts, each with variance 1/2. Equivalently, $\phi_{ms,j}(i)$ is a stationary and ergodic stochastic fading process that is independent for each sender and receiver antenna pair, where $E_\phi[\phi_{ms,j}(i)\,\phi^*_{ms,j}(i)] = E_\phi[|\phi_{ms,j}(i)|^2] = 1$. The fading coefficients can also be given in matrix notation, i.e., $\phi_{ms,j}(i) = (\mathbf{\Phi}_j(i))_{ms}$. Thus, $\mathbf{\Phi}_j(i)$ is an $M \times L_i$ matrix of complex variates whose columns are independently normally distributed with mean vector $\mathbf{0}$ and covariance matrix $\mathbf{\Psi}_j(i) = \mathbf{I}_M\ \forall(i,j)$, i.e., $N(\mathbf{0}, \mathbf{I}_M)$ [29]. Consequently, $\mathbf{\Phi}_j(i)\mathbf{\Phi}_j^\dagger(i)$ is a positive definite Hermitian matrix having the complex Wishart distribution characterized by the following probability density function [29]

$$f(\mathbf{\Phi}_j(i)\mathbf{\Phi}_j^\dagger(i)) = \frac{e^{-tr[\mathbf{\Psi}_j^{-1}(i)\mathbf{\Phi}_j(i)\mathbf{\Phi}_j^\dagger(i)]}\{\det[\mathbf{\Phi}_j(i)\mathbf{\Phi}_j^\dagger(i)]\}^{L_i - M}}{\pi^{\frac{1}{2}M(M-1)}\{\det[\mathbf{\Psi}_j(i)]\}^{L_i}\prod_{k=1}^{M}\Gamma(L_i - k + 1)}. \tag{7}$$

This complex Wishart distribution for a matrix $\mathbf{\Phi}_j(i)\mathbf{\Phi}_j^\dagger(i)$ will be denoted by $\mathbf{\Phi}_j(i)\mathbf{\Phi}_j^\dagger(i) \sim \mathcal{W}_M(L_i, \mathbf{\Psi}_j(i))$.

3. Receiver (uplink) ergodic capacity

Let $\mathbf{H}_j(0)$ represent the channel matrix for cell 0, i.e., $\mathbf{H}_j(0)$ describes the channel matrix to receiver node j from the nodes in the same cell as j is located. The analysis is asymptotic in n, i.e., $n \to \infty$. Therefore, $A_T(n) \to \infty$, and wolog, we consider that the cell 0 is located at the center of the network area. Given that each node transmits to another node with power P using only one antenna, and CSI is only known at the receiver side, the ergodic capacity of a receiving node j is given (in units of bits/s/Hz) by [2,1,6,7]

$$C_j = \frac{1}{9}E_{\mathbf{H}}\left\{\log_2\det\left[\mathbf{I}_M + P\mathbf{H}_j(0)\mathbf{H}_j^\dagger(0)\left(\sigma_{\mathbf{z}}^2\mathbf{I}_M + \sum_{i\geqslant 1}P\mathbf{H}_j(i)\mathbf{H}_j^\dagger(i)\right)^{-1}\right]\right\}, \tag{8}$$

where the term $\frac{1}{9}$ accounts for the FDMA, $E_{\mathbf{H}}[\cdot]$ denotes the ergodic expectation over all instantaneous $\mathbf{H}_j(i)$, and the summation in i refers to the interference coming from all cells in the network using the same frequency band ΔW as j uses for reception.

3.1. Upper bound computation

From (8), noting that $\log_2\det(\cdot)$ is concave and using Jensen's inequality and the fact that, given $j, \mathbf{H}_j(i)$ is independently distributed for all i, we obtain

$$C_j \leqslant \frac{1}{9}\log_2\det\left\{\mathbf{I}_M + PE_{\mathbf{H}}[\mathbf{H}_j(0)\mathbf{H}_j^\dagger(0)]E_{\mathbf{H}}\left[\left(\sigma_{\mathbf{z}}^2\mathbf{I}_M + P\sum_{i\geqslant 1}\mathbf{H}_j(i)\mathbf{H}_j^\dagger(i)\right)^{-1}\right]\right\}. \tag{9}$$

First, we compute the data signal strength.

3.1.1. Data signal strength computation

Because $\mathbf{H}_j(0)$ is an $M \times L_0$ matrix with independent and identically distributed (iid) zero mean unit variance entries, we have that

$$E_{\mathbf{H}}[\mathbf{H}_j(0)\mathbf{H}_j^\dagger(0)] = diag\left(E_h\left[\sum_{s=1}^{L_0}h_{1s,j}(0)h^*_{1s,j}(0)\right], \ldots, E_h\left[\sum_{s=1}^{L_0}h_{Ms,j}(0)h^*_{Ms,j}(0)\right]\right). \tag{10}$$

Because the distance between the transmit antenna from any other node and each receiving antenna in node j is assumed to be the same, we obtain

$$E_h\left[\sum_{s=1}^{L_0}h_{ms,j}(0)h^*_{ms,j}(0)\right] = E_{S,\phi,r}\left[\sum_{s=1}^{L_0}\frac{\phi_{ms,j}(0)\phi^*_{ms,j}(0)}{(1 + r_{s,j}(0))^{2\alpha}}\right] = E_{S,r}\left[\sum_{s=1}^{L_0}\frac{1}{(1 + r_{s,j}(0))^{2\alpha}}\right], \tag{11}$$

for $1 \leqslant m \leqslant M$. Note that the expectation for the channel matrix is carried for three different parameters due to mobility of the nodes in the network, namely, fading coefficients, the distance between sender and receiver, and the number of sender nodes. Substituting (11) in (10), we have

$$E_{\mathbf{H}}[\mathbf{H}_j(0)\mathbf{H}_j^{\dagger}(0)] = E_{S,r}\left[\sum_{s=1}^{L_0}\frac{1}{\left(1+r_{s,j}(0)\right)^{2\alpha}}\right]\mathbf{I}_M. \tag{12}$$

Lemma 1. *For the uniform mobility model,*

$$E_{S,r}\left[\sum_{s=1}^{L_0}\frac{1}{\left(1+r_{s,j}(0)\right)^{2\alpha}}\right] = q(\mathcal{A},\rho a_{cell})\,g(a_{cell},\alpha), \tag{13}$$

where $g(a_{cell},\alpha)=\frac{4}{a_{cell}}\left[\frac{\left(1+\sqrt{\frac{a_{cell}}{2}}\right)^{2\alpha-1}-1-\sqrt{\frac{a_{cell}}{2}}(2\alpha-1)}{(2\alpha-2)(2\alpha-1)\left(1+\sqrt{\frac{a_{cell}}{2}}\right)^{2\alpha-1}}\right]$ *and*

$$q(\mathcal{A},\rho a_{cell}) := \frac{\mathcal{A}(\mathcal{A}+1)\Gamma(\mathcal{A}+1,\rho a_{cell})+(\rho a_{cell}+e^{-\rho a_{cell}}-1-\mathcal{A})\Gamma(\mathcal{A}+2)-\frac{(\rho a_{cell})^{\mathcal{A}+2}\,{}_2F_2(2;\mathcal{A}+3;\rho a_{cell})e^{-\rho a_{cell}}}{\mathcal{A}+2}}{\Gamma(\mathcal{A}+2)} + (\mathcal{A}-1)\left[1-\frac{\Gamma(\mathcal{A}+1,\rho a_{cell})}{\Gamma(\mathcal{A}+1)}\right],$$

in which ${}_2F_2(\cdot;\cdot;\cdot)$ *is used to denote the generalized hypergeometric function [29].*

Proof. Because the steady-state node distribution is uniform, the distances between the nodes in cell 0 and node j are iid distributed. Therefore,

$$E_{S,r}\left[\sum_{s=1}^{L_0}\frac{1}{\left(1+r_{s,j}(0)\right)^{2\alpha}}\right] = \sum_{s_0=2}^{\infty}L_0\,\mathbb{P}\{S=s_0\}\int_0^{r_m}\frac{f_R(r)dr}{(1+r)^{2\alpha}}, \tag{14}$$

where $f_R(r)$ is the probability density function for the distance between a sender node and node j in cell 0, and r_m is their maximum distance. For a uniform node distribution and considering node j located at the center of cell 0 (for a circular cell shape), we have that [30]

$$f_R(r)=\begin{cases}\frac{2r}{r_m^2} & \text{if } 0\leqslant r\leqslant r_m,\\ 0 & \text{otherwise.}\end{cases} \tag{15}$$

This assumption is justified by observing that the square cell arrangement in Fig. 1 can be circumvented by a circle for the purpose of upper bound computation. Besides, the analytical results will be contrasted with Monte-Carlo simulations for the actual ergodic capacity. Noting that the maximum possible distance inside a cell between the receiver node (assumed to be placed at the center of the cell) and another node is $\sqrt{\frac{a_{cell}}{2}}$, we obtain the following result

$$\int_0^{r_m}\frac{2rdr}{r_m^2(1+r)^{2\alpha}}=\frac{4}{a_{cell}}\int_0^{\sqrt{\frac{a_{cell}}{2}}}\frac{rdr}{(1+r)^{2\alpha}}=\frac{4}{a_{cell}}\left[\frac{\left(1+\sqrt{\frac{a_{cell}}{2}}\right)^{2\alpha-1}-1-\sqrt{\frac{a_{cell}}{2}}(2\alpha-1)}{(2\alpha-2)(2\alpha-1)\left(1+\sqrt{\frac{a_{cell}}{2}}\right)^{2\alpha-1}}\right]. \tag{16}$$

Now, from (3), the summation term in (14) becomes

$$\begin{aligned}\sum_{s_0=2}^{\infty}L_0\,\mathbb{P}\{S=s_0\} &= \sum_{s_0=2}^{\infty}\frac{L_0}{s_0!}(\rho a_{cell})^{s_0}e^{-\rho a_{cell}} = e^{-\rho a_{cell}}\left[\sum_{s_0=2}^{\mathcal{A}}\frac{s_0-1}{s_0!}(\rho a_{cell})^{s_0}+(\mathcal{A}-1)\sum_{s_0=\mathcal{A}+1}^{\infty}\frac{1}{s_0!}(\rho a_{cell})^{s_0}\right]\\ &= \frac{\mathcal{A}(\mathcal{A}+1)\Gamma(\mathcal{A}+1,\rho a_{cell})+(\rho a_{cell}+e^{-\rho a_{cell}}-1-\mathcal{A})\Gamma(\mathcal{A}+2)-\frac{(\rho a_{cell})^{\mathcal{A}+2}\,{}_2F_2(2;\mathcal{A}+3;\rho a_{cell})e^{-\rho a_{cell}}}{\mathcal{A}+2}}{\Gamma(\mathcal{A}+2)}\\ &\quad+(\mathcal{A}-1)\left[1-\frac{\Gamma(\mathcal{A}+1,\rho a_{cell})}{\Gamma(\mathcal{A}+1)}\right].\end{aligned} \tag{17}$$

Combining 14, 16 and 17, the final result follows. □

3.1.2. Interference computation

The interference is computed in three cases given by the amount of interference experienced by a node, which in turn is a function of the transmit power level P: strong interference (noise is negligible), no interference (noise is dominant), and the intermediate case. The intermediate case is computed in this subsection.

To compute the interference, we need the following Lemma and Corollary.

Lemma 2. *Let the same order square Hermitian matrices* $\mathbf{G}$ *and* $\mathbf{V}$ *be positive definite. Then*

$$(\mathbf{G}+\mathbf{V})^{-1}\leqslant\frac{1}{4}(\mathbf{G}^{-1}+\mathbf{V}^{-1}), \tag{18}$$

with equality if and only if $\mathbf{G}=\mathbf{V}$.

Proof. See Theorems 6.6 and 6.7 in page 168 [31].

Corollary 1. *Let the square Hermitian matrix* $\mathbf{Y}(i)$ *be positive definite, where* $i \in [1,\infty)$ *and* $\mathbf{Y}(i)$ *has same order for all i. Then*

$$\left(\sum_{i=1}^{\infty}\mathbf{Y}(i)\right)^{-1} \leqslant \sum_{i=1}^{\infty}\frac{1}{4^i}\mathbf{Y}^{-1}(i), \tag{19}$$

with equality if and only if $\mathbf{Y}(i)=\sum_{k=i+1}^{\infty}\mathbf{Y}(k)\ \forall i \geqslant 1$.

Proof. In Lemma 2, put $\mathbf{G}=\mathbf{Y}(i),\ \mathbf{V}=\sum_{k=i+1}^{\infty}\mathbf{Y}(k)$, and the result follows. □

From (9) and Lemma 2, we obtain

$$C_j \leqslant \frac{1}{9}\log_2\det\left\{\mathbf{I}_M + PE_{\mathbf{H}}[\mathbf{H}_j(0)\mathbf{H}_j^{\dagger}(0)]\left[\frac{1}{4\sigma_{\mathbf{z}}^2}\mathbf{I}_M + \frac{1}{4P}E_{\mathbf{H}}\left(\sum_{i\geqslant 1}\mathbf{H}_j(i)\mathbf{H}_j^{\dagger}(i)\right)^{-1}\right]\right\}. \tag{20}$$

An upper bound on the capacity of the proposed scheme can be obtained by considering the distance between the receiver node j in cell 0 and the interferer in cell i equals the distance from the farthest corner of the interfering cell. However, as it will be evident in Section 4, an analytical expression for the capacity of the MIMO MANET when the interfering nodes are at the center of cells provides a closer fit with the results obtained by Monte-Carlo simulations when nodes are randomly distributed in each cell. Hence, to simplify our derivations of interference, we assume that the distance between the receiver node j in cell 0 and the interferer in cell i equals distance from center to center of these two cells. Accordingly, due to the cell arrangement illustrated in Fig. 1, the path loss from each interfering cell using the same frequency band ΔW as j can be written by [4]

$$\frac{1}{(1+r_j(i))^{\alpha}} = \frac{1}{\left[1+\sqrt{(3\sqrt{a_{cell}}\,k_i)^2+(3\sqrt{a_{cell}}\,\ell_i)^2}\right]^{\alpha}} = \frac{1}{\left(1+3\sqrt{a_{cell}}\sqrt{k_i^2+\ell_i^2}\right)^{\alpha}}, \tag{21}$$

where $(3\sqrt{a_{cell}}\,k_i, 3\sqrt{a_{cell}}\,\ell_i)$ are the coordinates of cell i with respect to cell 0 (i.e., cell 0 is taken as the origin for the coordinates), in which $k_i \in \mathbb{Z}$ and $\ell_i \in \mathbb{Z}$, and both k_i and ℓ_i cannot be zero simultaneously. Consequently,

$$\mathbf{H}_j(i)\mathbf{H}_j^{\dagger}(i) = \frac{1}{(1+r_j(i))^{2\alpha}}\mathbf{\Phi}_j(i)\mathbf{\Phi}_j^{\dagger}(i) = \frac{1}{\left(1+3\sqrt{a_{cell}}\sqrt{k_i^2+\ell_i^2}\right)^{2\alpha}}\mathbf{\Phi}_j(i)\mathbf{\Phi}_j^{\dagger}(i). \tag{22}$$

The following lemma is used to compute interference in (20).

Lemma 3. *Let* $\mathbf{G}\sim\mathcal{W}_p(t,\mathbf{\Psi})$. *Then, for* $t-p>0$

$$E[\mathbf{G}^{-1}] = \frac{1}{t-p}\,\mathbf{\Psi}^{-1}. \tag{23}$$

Proof. See [32,33] considering the complex Wishart distribution given in (7).

From (22), Corollary 1 and Lemma 3, the total interference in (20) can be computed as

$$\begin{aligned} E_{\mathbf{H}}\left(\sum_{i\geqslant 1}\mathbf{H}_j(i)\mathbf{H}_j^{\dagger}(i)\right)^{-1} &\leqslant \sum_{i\geqslant 1}\frac{1}{4^i}E_{\mathbf{\Phi}}\left\{\left[\frac{1}{(1+r_j(i))^{2\alpha}}\mathbf{\Phi}_j(i)\mathbf{\Phi}_j^{\dagger}(i)\right]^{-1}\right\} = \sum_{i\geqslant 1}\frac{(1+r_j(i))^{2\alpha}}{4^i}E_S\left[\frac{1}{L_i-M}\right]\mathbf{\Psi}_j^{-1}(i) \\ &= \underbrace{E_S\left[\frac{1}{L_i-M}\right]}_{\zeta(\rho,a_{cell},M,\mathcal{A})}\underbrace{\sum_{k_i\in\mathbb{Z}}\sum_{\ell_i\in\mathbb{Z}}\frac{\left(1+3\sqrt{a_{cell}}\sqrt{k_i^2+\ell_i^2}\right)^{2\alpha}}{4^i}}_{u_1(a_{cell},\alpha)}\mathbf{I}_M = \zeta(\rho,a_{cell},M,\mathcal{A})\,u_1(a_{cell},\alpha)\,\mathbf{I}_M : \\ &= w_1(\rho,a_{cell},\alpha,M,\mathcal{A})\,\mathbf{I}_M, \end{aligned} \tag{24}$$

where we used the fact that $\mathbf{\Psi}_j(i)=\mathbf{I}_M\forall(i,j)$, and $\forall i$

[4] In this case, $r_j(i)$ is the distance between the center of cell i and the center of the cell in which j is currently located (i.e., cell 0).

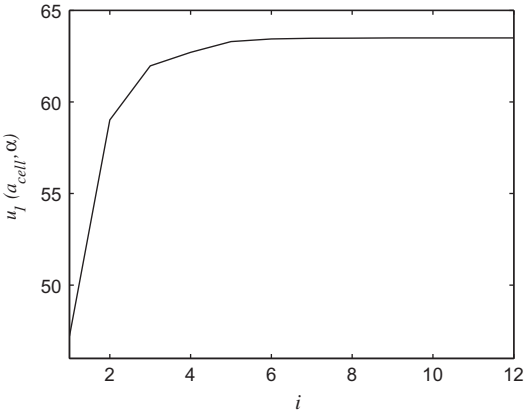

Fig. 4. Convergence of $u(a_{cell},\alpha)$ as a function of cell i, for $a_{cell} = 2$ m^2 and $\alpha = 2$.

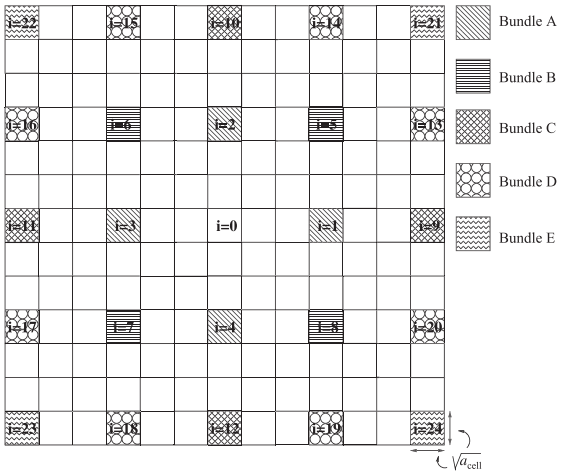

Fig. 5. Cell classification for bundling Wishart matrices for tight upper bound computation.

$$\zeta(\rho, a_{cell}, M, \mathcal{A}) := E_S\left[\frac{1}{L_i - M}\right] = e^{-\rho\, a_{cell}}\left[\sum_{s_i=M+2}^{\mathcal{A}} \frac{(\rho\, a_{cell})^{s_i}}{[s_i - 1 - M]s_i!} + \frac{1}{\mathcal{A} - 1 - M}\sum_{s_i=\mathcal{A}+1}^{\infty} \frac{(\rho\, a_{cell})^{s_i}}{s_i!}\right]$$
$$= (\rho a_{cell})^{M+2} e^{-\rho\, a_{cell}}\left[\frac{{}_2F_2(1,1;2,M+3;\rho a_{cell})}{\Gamma(M+3)} - \frac{(\rho a_{cell})^{\mathcal{A}-1-M}\,{}_2F_2(1,\mathcal{A}-M;\mathcal{A}+2;\mathcal{A}+1-M)}{(\mathcal{A}-M)\Gamma(\mathcal{A})}\right]$$
$$+ \frac{1}{\mathcal{A}-1-M}\left[1 - \frac{\Gamma(\mathcal{A}+1,\rho a_{cell})}{\Gamma(\mathcal{A}+1)}\right]. \tag{25}$$

The function w_1 is used later to obtain one bound for the capacity of the distributed MIMO ad hoc network. The function $u_1(a_{cell},\alpha)$ in (24) represents the effect of interfering nodes from different cells. This function converges very fast, as illustrated in Fig. 4. This result demonstrates that only adjacent interfering cells are dominant, which is commonly considered for medium access control (MAC) protocol design [34].[5]

3.1.3. Interference analysis for a tighter upper bound

We can use the above derivations to compute interference for a tighter bound for the capacity of MIMO MANETs. We observe that the interfering nodes for cell 5 in the center of Fig. 1 are those located inside of the other cells also numbered 5, which are symmetrically located in the network. To clarify our next approach, consider Fig. 5 which is obtained from Fig. 1 by taking at most only those cells that are two hops away [34] and can interfere with the center cell (designated as cell 0). Accordingly, we can bundle the set of symmetric cells in the computation of (20) to obtain a tighter bound, because the channel matrix associated with these interfering cells are equivalent on the average, for a uniform distribution of the nodes.

[5] It is commonly known that the major portion of interference is caused by two adjacent hops in wireless ad hoc networks [34].

Consequently, consider the following bundling and respective associated distances to receiver node j in cell 0. $\mathbf{A} = \sum_{i=1}^{4} \mathbf{\Phi}_j(i)\mathbf{\Phi}_j^{\dagger}(i)$ with $r_j(\mathbf{A}) = 3\sqrt{a_{cell}}$, $\mathbf{B} = \sum_{i=5}^{8} \mathbf{\Phi}_j(i)\mathbf{\Phi}_j^{\dagger}(i)$ with $r_j(\mathbf{B}) = 3\sqrt{2a_{cell}}$, $\mathbf{C} = \sum_{i=9}^{12} \mathbf{\Phi}_j(i)\mathbf{\Phi}_j^{\dagger}(i)$ with $r_j(\mathbf{C}) = 6\sqrt{a_{cell}}$, $\mathbf{D} = \sum_{i=13}^{20} \mathbf{\Phi}_j(i)\mathbf{\Phi}_j^{\dagger}(i)$ with $r_j(\mathbf{D}) = 3\sqrt{5a_{cell}}$, $\mathbf{E} = \sum_{i=21}^{24} \mathbf{\Phi}_j(i)\mathbf{\Phi}_j^{\dagger}(i)$ with $r_j(\mathbf{E}) = 6\sqrt{2a_{cell}}$, and consider the following lemma.

Lemma 4. *Let* $\mathbf{G}(1), \ldots, \mathbf{G}(K)$ *be independently distributed with* $\mathbf{G}(i) \sim \mathcal{W}_p(q_i, \mathbf{\Psi})$ *for* $i = 1, \ldots, K$. *Then* $\sum_{i=1}^{K} \mathbf{G}(i) \sim \mathcal{W}_p(\sum_{i=1}^{K} q_i, \mathbf{\Psi})$.

Proof. The results follows from Theorem 3.3.8 in page 94 [35].

Using Lemma 4, because the steady-state node distribution is uniform, it results that $\mathbf{A}, \mathbf{B}, \mathbf{C}$ and $\mathbf{E}$ are iid with distribution $\mathcal{W}_M(\sum_{i=1}^{4} L_i, \mathbf{I}_M)$, and $\mathbf{D} \sim \mathcal{W}_M(\sum_{i=13}^{20} L_i, \mathbf{I}_M)$. From (20), Corollary 1 and Lemma 4, we obtain for two hops

$$
\begin{aligned}
E_{\mathbf{H}}\left(\sum_{i=1}^{24} \mathbf{H}_j(i)\mathbf{H}_j^{\dagger}(i)\right)^{-1} &= E_{\mathbf{\Phi}}\left[\frac{\mathbf{A}}{(1+r_j(\mathbf{A}))^{2\alpha}} + \frac{\mathbf{B}}{(1+r_j(\mathbf{B}))^{2\alpha}} + \frac{\mathbf{C}}{(1+r_j(\mathbf{C}))^{2\alpha}} + \frac{\mathbf{D}}{(1+r_j(\mathbf{D}))^{2\alpha}} + \frac{\mathbf{E}}{(1+r_j(\mathbf{E}))^{2\alpha}}\right]^{-1} \\
&\leqslant E_{\mathbf{\Phi}}[\mathbf{A}^{-1}] \underbrace{\left[\frac{(1+3\sqrt{a_{cell}})^{2\alpha}}{4} + \frac{(1+3\sqrt{2a_{cell}})^{2\alpha}}{16} + \frac{(1+3\sqrt{4a_{cell}})^{2\alpha}}{64} + \frac{(1+3\sqrt{8a_{cell}})^{2\alpha}}{1024}\right]}_{u_2(a_{cell},\alpha)} \\
&+ E_{\mathbf{\Phi}}[\mathbf{D}^{-1}] \underbrace{\frac{(1+3\sqrt{5a_{cell}})^{2\alpha}}{256}}_{u_3(a_{cell},\alpha)} = u_2(a_{cell},\alpha) \sum_{S_1 > \frac{M}{4}+1} \sum_{S_2 > \frac{M}{4}+1} \sum_{S_3 > \frac{M}{4}+1} \sum_{S_4 > \frac{M}{4}+1} \frac{\prod_{i=1}^{4} \mathbb{P}\{S = S_i\}}{\sum_{i=1}^{4} \min(\mathcal{A}, S_i) - 4 - M} \mathbf{I}_M \\
&+ u_3(a_{cell},\alpha) \sum_{S_{13} > \frac{M}{8}+1} \sum_{S_{14} > \frac{M}{8}+1} \cdots \sum_{S_{20} > \frac{M}{8}+1} \frac{\prod_{i=13}^{20} \mathbb{P}\{S = S_i\}}{\sum_{i=13}^{20} \min(\mathcal{A}, S_i) - 8 - M} \mathbf{I}_M := w_2(\rho, a_{cell}, \alpha, M, \mathcal{A})\mathbf{I}_M, \qquad (26)
\end{aligned}
$$

where $\mathbb{P}\{S = S_i\}$ is given by (3) $\forall i$, and we used the fact that $E_{\mathbf{\Phi}}[\mathbf{A}^{-1}] = E_{\mathbf{\Phi}}[\mathbf{B}^{-1}] = E_{\mathbf{\Phi}}[\mathbf{C}^{-1}] = E_{\mathbf{\Phi}}[\mathbf{E}^{-1}]$.

We also show this by comparing our analytical results with Monte-Carlo simulation of (8) to demonstrate the tightness of this capacity upper bound. One may naively expect that this new bound should be higher than the first capacity bound because we ignore the effect of interference from nodes located more than two hops away. However, the new bundling allows to increase the effect of adjacent nodes while ignoring the influence of farther nodes, corroborating the common belief that only adjacent nodes have the major effect on the value of the signal-to-noise and interference ratio (SNIR) and capacity [34].

3.1.4. Capacity upper bound

The ergodic capacity of a receiver node j follows from (20), (12), Lemma 1, and either (24) or (26). Hence,

$$
\begin{aligned}
C_j &\leqslant \frac{1}{9}\log_2 \det\left\{\left[1 + Pq(\mathcal{A}, \rho a_{cell})g(a_{cell},\alpha)\left(\frac{1}{4\sigma_{\mathbf{z}}^2} + \frac{w(\rho, a_{cell}, \alpha, M, \mathcal{A})}{4P}\right)\right]\mathbf{I}_M\right\} \\
&= \frac{M}{9}\log_2\left[1 + Pq(\mathcal{A}, \rho a_{cell})g(a_{cell},\alpha)\left(\frac{1}{4\sigma_{\mathbf{z}}^2} + \frac{w(\rho, a_{cell}, \alpha, M, \mathcal{A})}{4P}\right)\right], \qquad (27)
\end{aligned}
$$

where the function $w(\rho, a_{cell}, \alpha, M, \mathcal{A})$ represents either w_1 or w_2 from (24) or (26), respectively.

For the case of no interference, the upper-bound capacity is obtained from (9) and (27), where the term associated with interference is ignored. Accordingly, we have

$$
C_j \leqslant \frac{M}{9}\log_2\left[1 + \frac{P}{\sigma_{\mathbf{z}}^2} q(\mathcal{A}, \rho a_{cell})g(a_{cell},\alpha)\right]. \qquad (28)
$$

On the other hand, if interference is strong, the term associated with noise is neglected. In such case, we obtain

$$
C_j \leqslant \frac{M}{9}\log_2[1 + q(\mathcal{A}, \rho a_{cell})g(a_{cell},\alpha)\, w(\rho, a_{cell}, \alpha, M, \mathcal{A})]. \qquad (29)
$$

Therefore, from (27)–(29), the node upper bound capacity grows linearly with the number of receiving antennas M. Furthermore, because the terms in these equations do not depend on n, the upper bound capacity does not decrease with n. Note that our channel matrix $\mathbf{H}_j(i)$ incorporates the decay with distance, i.e., $\frac{1}{(1+r_j(i))^{\alpha}}$, which is the large-scale representation of the channel and that causes the interference to decay with distance.

3.2. Lower bound computation

We assume that the rank of $\mathbf{H}_j(i)$ matrix is M.[6] Therefore, $\mathbf{H}_j(i)\mathbf{H}_j^{\dagger}(i)$ is a full rank matrix. Also in Section 2, we assumed that distances between the transmitting node s and all M antennas of the receiver j are equal. Accordingly, we can decompose

[6] We choose the network parameters such that the probability of L_i be smaller than M is close to zero.

$\mathbf{H}_j(i) = \mathbf{\Phi}_j(i)\mathbf{D}_j(i)$ where $\mathbf{D}_j(i)$ is defined as the diagonal matrix $diag\left[\frac{1}{(1+r_{j,1}(i))^{\alpha}}, \frac{1}{(1+r_{j,2}(i))^{\alpha}}, \ldots, \frac{1}{(1+r_{j,L_i}(i))^{\alpha}}\right]$ and $\mathbf{\Phi}_j(i)$ is a M by L_i matrix whose elements are $\phi_{ms,j}(i)$ (see Section 2.4). Thus, we have $\mathbf{H}_j(i)\mathbf{H}_j^{\dagger}(i) = \mathbf{\Phi}_j(i)\mathbf{D}_j^2(i)\mathbf{\Phi}_j(i)^{\dagger}$. Since the number of transmit nodes, L_i, and the channel coefficients are independent variables, we can rewrite (8) as

$$C_j = \frac{1}{9}E_{L_i}\left\{E_{\mathbf{\Phi},r}\left[\log_2 \det\left(\mathbf{I_M} + P\mathbf{\Phi}_j(0)\mathbf{D}_j^2(0)\mathbf{\Phi}_j^{\dagger}(0)\mathbf{P}_{\mathbf{in}}^{-1}\right)\right]\right\}, \tag{30}$$

where $\mathbf{P_{in}} = \sigma_z^2\mathbf{I_M} + \sum_{i\geqslant 1} P\mathbf{H}_j(i)\mathbf{H}_j^{\dagger}(i) = \sigma_z^2\mathbf{I_M} + \sum_{i\geqslant 1} P\mathbf{\Phi}_j(i)\mathbf{D}_j^2(i)\mathbf{\Phi}_j(i)^{\dagger}$.

Now in order to derive the lower bound of C_j in (30), we first compute the lower bound of the following expression

$$C_j(\mathbf{\Phi}) = \frac{1}{9}E_{\mathbf{\Phi},r}\left[\log_2 \det\left(\mathbf{I_M} + P\mathbf{\Phi}_j(0)\mathbf{D}_j^2(0)\mathbf{\Phi}_j^{\dagger}(0)\mathbf{P}_{\mathbf{in}}^{-1}\right)\right]. \tag{31}$$

Lemma 5. *The ergodic capacity in (31) is lower bounded by*

$$C_j(\mathbf{\Phi}) \geqslant \frac{1}{9}E_{\mathbf{\Phi}}\left[\log_2 \det\left(\mathbf{I_M} + c_3 P\mathbf{\Phi}_j(0)\mathbf{\Phi}_j^{\dagger}(0)\mathbf{P}_{\mathbf{in}^{\natural}-1}\right)\right], \tag{32}$$

where $\mathbf{P}_{\mathbf{in}}^{\natural} = \sigma_z^2\mathbf{I_M} + \sum_{i\geqslant 1}\frac{P}{(1+r_{min}(i))^{2\alpha}}\mathbf{\Phi}_j(i)\mathbf{\Phi}_j^{\dagger}(i)$ *and* $c_3 := \left(1+\sqrt{a_{cell}/2}\right)^{-2\alpha}$ *is a constant determined by* a_{cell} *and* α.

Proof. The elements of the diagonal matrix $\mathbf{D}_j^2(0)$ in (31) are $\frac{1}{(1+r_{s,j}(0))^{2\alpha}}$. Now let's define the diagonal matrix $\mathbf{D}_{jmin}^2(0)$ where it has $\frac{1}{(1+r_{max})^{2\alpha}}$ for its element and $r_{max} \geqslant r_{s,j}(0)$ for all values of s and j. This corresponds to the large scale path loss gain when the transmitting nodes in the cell 0 are transmitting at the farthest distance. Since we can place the receiver node at the center of the cell for the computation of capacity, the maximum distance in a cell between the receiver node and other nodes is $\sqrt{a_{cell}/2}$. Now let's define the matrix $\mathbf{\Phi}_j(0)\{\mathbf{D}_j^2(0) - \mathbf{D}_{jmin}^2(0)\}\mathbf{\Phi}_j^{\dagger}(0)$. Because all elements in $\{\mathbf{D}_j^2(0) - \mathbf{D}_{jmin}^2(0)\}$ have positive values, then $\mathbf{\Phi}_j(0)\{\mathbf{D}_j^2(0) - \mathbf{D}_{jmin}^2(0)\}\mathbf{\Phi}_j^{\dagger}(0)$ is a positive semi-definite matrix. Thus, we have

$$\mathbf{\Phi}_j(0)\mathbf{D}_j^2(0)\mathbf{\Phi}_j^{\dagger}(0) \geqslant \mathbf{\Phi}_j(0)\mathbf{D}_{jmin}^2(0)\mathbf{\Phi}_j^{\dagger}(0). \tag{33}$$

Similarly, $\mathbf{H}_j(i)\mathbf{H}_j^{\dagger}(i)$ in $\mathbf{P_{in}}$ can be decomposed into $\mathbf{\Phi}_j(i)\mathbf{D}_j^2(i)\mathbf{\Phi}_j^{\dagger}(i)$. Since each element in the diagonal matrix $\mathbf{D}_j^2(i)$ is defined as $\frac{1}{(1+r_{s,j}(i))^{2\alpha}}$, we conclude that

$$\sum_{i\geqslant 1}\mathbf{\Phi}_j(i)\mathbf{D}_j^2(i)\mathbf{\Phi}_j^{\dagger}(i) \leqslant \sum_{i\geqslant 1}\mathbf{\Phi}_j(i)\mathbf{D}_{jmax}^2(i)\mathbf{\Phi}_j^{\dagger}(i), \tag{34}$$

where $\mathbf{D}_{jmax}^2(i)$ is a diagonal matrix which elements are defined as $\frac{1}{(1+r_{min}(i))^{2\alpha}}$ and $r_{min}(i) \leqslant r_{s,j}(i)$ for all values of s and j.

Thus, $\mathbf{P}_{\mathbf{in}}^{\natural}$ can be defined as

$$\begin{aligned}\mathbf{P}_{\mathbf{in}}^{\natural} &= \sigma_z^2\mathbf{I_M} + \sum_{i\geqslant 1}\mathbf{\Phi}_j(i)\mathbf{D}_{jmax}^2(i)\mathbf{\Phi}_j^{\dagger}(i) = \sigma_z^2\mathbf{I_M} + \sum_{i\geqslant 1}\mathbf{\Phi}_j(i)\frac{P}{(1+r_{min}(i))^{2\alpha}}\cdot\mathbf{I}_{L_i}\mathbf{\Phi}_j^{\dagger}(i)\\ &= \sigma_z^2\mathbf{I_M} + \sum_{i\geqslant 1}\frac{P}{(1+r_{min}(i))^{2\alpha}}\mathbf{\Phi}_j(i)\mathbf{\Phi}_j^{\dagger}(i).\end{aligned} \tag{35}$$

Finally, (32) can be written as

$$C_j(\mathbf{\Phi}) \geqslant \frac{1}{9}E_{\mathbf{\Phi}}\log_2 \det\left(\mathbf{I_M} + P\mathbf{\Phi}_j(0)\mathbf{D}_{jmin}^2(0)\mathbf{\Phi}_j^{\dagger(0)}\mathbf{P}_{\mathbf{in}}^{\natural-1}\right). \tag{36}$$

By replacing $\mathbf{D}_{jmin}(0)$ with $\frac{1}{\left(1+\sqrt{a_{cell}/2}\right)^{2\alpha}}\mathbf{I}_{L_0}$, the proof follows immediately. □

Based on Minkowski's inequality [36], which is $[\det(\mathbf{A}+\mathbf{B})]^{\frac{1}{n}} \geqslant [\det(\mathbf{A})]^{\frac{1}{n}} + [\det(\mathbf{B})]^{\frac{1}{n}}$ when $\mathbf{A}$ and $\mathbf{B}$ are $n\times n$ matrices, (32) can be further simplified as

$$\begin{aligned}C_j(\mathbf{\Phi}) &\geqslant \frac{M}{9}E_{\mathbf{\Phi}}\left\{\log_2\left[\det\left(\mathbf{I_M} + c_3P\mathbf{\Phi}_j(0)\mathbf{\Phi}_j^{\dagger}(0)\mathbf{P}_{\mathbf{in}}^{\natural\ -1}\right)\right]^{\frac{1}{M}}\right\}\\ &\geqslant \frac{M}{9}E_{\mathbf{\Phi}}\left\{\log_2\left[[\det(\mathbf{I_M})]^{\frac{1}{M}} + \left[\det\left(c_3P\mathbf{\Phi}_j(0)\mathbf{\Phi}_j^{\dagger}(0)\mathbf{P}_{\mathbf{in}}^{\natural\ -1}\right)\right]^{\frac{1}{M}}\right]\right\}\\ &= \frac{M}{9}E_{\mathbf{\Phi}}\left\{\log_2\left[1+\exp\left(\frac{1}{M}\ln\det\left(c_3P\mathbf{\Phi}_j(0)\mathbf{\Phi}_j^{\dagger}(0)\mathbf{P}_{\mathbf{in}}^{\natural\ -1}\right)\right)\right]\right\}.\end{aligned} \tag{37}$$

Since, from Jensen's inequality, $E_{\mathbf{\Phi}}[\log_2(1+a\exp(x))]$ is a convex function for $a \geqslant 0$, we arrive at

$$C_j(\mathbf{\Phi}) \geqslant \frac{M}{9}\log_2\left\{1+\exp\left[E_{\mathbf{\Phi}}\left(\frac{1}{M}\ln\det\left(c_3 P\mathbf{\Phi}_j(0)\mathbf{\Phi}_j^{\dagger}(0)\mathbf{P}_{\mathbf{in}}^{\natural-1}\right)\right)\right]\right\}$$
$$\geqslant \frac{M}{9}\log_2\left\{1+P\exp\left[\frac{1}{M}E_{\mathbf{\Phi}}\ln\det\left(\mathbf{\Phi}_j(0)\mathbf{\Phi}_j^{\dagger(0)}\right)\right]-\frac{1}{M}E_{\mathbf{\Phi}}\ln\det\left(c_3^{-1}\mathbf{P}_{in}^{\natural}\right)\right\}. \tag{38}$$

For the last inequality, we used the properties $\det(\mathbf{A}\cdot\mathbf{B})=\det(\mathbf{A})\cdot\det(\mathbf{B})$ and $\det(\mathbf{A}^{-1})=\{\det(\mathbf{A})\}^{-1}$. From [37],

$$E_{\mathbf{\Phi}}\left[\ln\det\left(\mathbf{\Phi}_j(0)\mathbf{\Phi}_j^{\dagger}(0)\right)\right]=M(\ln 2-\gamma)+\sum_{j=1}^{M}\sum_{x=1}^{L_0-j}\frac{1}{x}, \tag{39}$$

where $L_0\geqslant M$ and $\gamma\approx 0.57721566$ is the Euler constant. Thus, by applying this to the last line of (38), we obtain

$$C_j(\mathbf{\Phi}) \geqslant \frac{M}{9}\log_2\left\{1+P\exp\left[(\ln 2-\gamma)+\frac{1}{M}\sum_{j\geqslant 1}^{M}\sum_{x=1}^{L_0-j}\frac{1}{x}-\frac{1}{M}E_{\mathbf{\Phi}}\left(\ln\det\left(c_3^{-1}\mathbf{P}_{\mathbf{in}}^{\natural}\right)\right)\right]\right\}. \tag{40}$$

Now we will prove the following lemma.

Lemma 6. $\frac{1}{M}\sum_{j=1}^{M}\sum_{x=1}^{L_0-j}\frac{1}{x}\geqslant\frac{1}{2}\ln\frac{M}{2}$.

Proof. We expand $\frac{1}{M}\sum_{j=1}^{M}\sum_{x=1}^{L_0-j}\frac{1}{x}$ as

$$\frac{1}{M}\sum_{j=1}^{M}\sum_{x=1}^{L_0-j}\frac{1}{x}=\frac{1}{M}\left(1+\frac{1}{2}+\frac{1}{3}+\ldots+\frac{1}{(L_0-1)}\right)+$$
$$\vdots$$
$$+\frac{1}{M}\left(1+\frac{1}{2}+\frac{1}{3}+\ldots+\frac{1}{(L_0-\frac{M}{2})}\right)+$$
$$\vdots$$
$$+\frac{1}{M}\left(1+\frac{1}{2}+\frac{1}{3}+\ldots+\frac{1}{(L_0-M)}\right). \tag{41}$$

For values of $M/2+1\leqslant j\leqslant M$, the terms in summation are positive because $L_0\geqslant M$ with high probability. Also, it is clear that for values of $1\leqslant j\leqslant M/2$, all the summations are greater than $\frac{1}{M}\sum_{x=1}^{L_0-M/2}\frac{1}{x}$. Thus we can write the following inequality,

$$\frac{1}{M}\sum_{j=1}^{M}\sum_{p=1}^{L_0-j}\frac{1}{x}\geqslant\frac{M}{2}\cdot\frac{1}{M}\sum_{x=1}^{L_0-M/2}\frac{1}{x}\;\Rightarrow\;\frac{1}{M}\sum_{j=1}^{M}\sum_{p=1}^{L_0-j}\frac{1}{x}\geqslant\frac{1}{2}\sum_{x=1}^{L_0-L_0/2}\frac{1}{x}. \tag{42}$$

From the definition of natural logarithm, we know that

$$\ln(a)=\int_1^a\frac{1}{x}\,dx\leqslant\sum_{x=1}^{a}\frac{1}{x}. \tag{43}$$

Thus, by applying (43) to (42), we have

$$\frac{1}{M}\sum_{j=1}^{M}\sum_{p=1}^{L_0-j}\frac{1}{x}\geqslant\frac{1}{2}\sum_{x=1}^{L_0/2}\frac{1}{x}\geqslant\frac{1}{2}\ln\frac{L_0}{2}\geqslant\frac{1}{2}\ln\frac{M}{2}, \tag{44}$$

which proves the lemma. □

Based on Lemma 6, we can rewrite (40) as

$$C_j(\mathbf{\Phi}) \geqslant \frac{M}{9}\log_2\left\{1+P\exp\left[(\ln 2-\gamma)+\frac{1}{2}\ln\frac{M}{2}-\frac{1}{M}E_{\mathbf{\Phi}}\left(\ln\det\left(c_3^{-1}\mathbf{P}_{\mathbf{in}}^{\natural}\right)\right)\right]\right\}$$
$$=\frac{M}{9}\log_2\left[1+\frac{\varphi(M,P,\gamma,\alpha,a_{cell})}{\exp\left(\frac{1}{M}E_{\mathbf{\Phi}}\left(\ln\det\mathbf{P}_{\mathbf{in}}^{\natural}\right)\right)}\right], \tag{45}$$

where $\varphi(M,P,\gamma,\alpha,a_{cell})=\frac{\sqrt{2M}P}{\exp\left(\gamma+\ln c_3^{-1}\right)}=\frac{\sqrt{2M}P}{\exp\left(\gamma+2\alpha\ln\left(1+\sqrt{a_{cell}/2}\right)\right)}$.

Since $\log\det(\cdot)$ is a concave function, based on Jensen's inequality we know that $E_{\mathbf{\Phi}}\ln\left(\det\mathbf{P}_{\mathbf{in}}^{\natural}\right)\leqslant\ln\det E_{\mathbf{\Phi}}\left(\mathbf{P}_{\mathbf{in}}^{\natural}\right)$. Hence, we have

$$C_j(\mathbf{\Phi}) \geqslant \frac{M}{9}\log_2\left\{1+\frac{\varphi(M,P,\gamma,\alpha,a_{cell})}{\exp\left[\frac{1}{M}\ln\det\left(E_{\mathbf{\Phi}}\left(\mathbf{P}_{\mathbf{in}}^{\natural}\right)\right)\right]}\right\}. \tag{46}$$

Lemma 7. *The ergodic lower bounded capacity in (46) can be reduced to*

$$C_j(\mathbf{\Phi}) \geqslant \frac{M}{9}\log_2\left[1+\frac{\varphi(M,P,\gamma,\alpha,a_{cell})}{\left(\sigma_z^2+\sum_{i\geqslant 1}\frac{L_iP}{(1+r_{min}(i))^{2\alpha}}\right)}\right]. \tag{47}$$

Proof. From the definition of $\mathbf{P}_{\mathbf{in}}^{\sharp}$ in (35), we have the following equation

$$E_{\mathbf{\Phi}}\left(\mathbf{P}_{\mathbf{in}}^{\sharp}\right)=E_{\mathbf{\Phi}}\left(\sigma_z^2\mathbf{I_M}+\sum_{i\geqslant 1}\frac{P\mathbf{\Phi}_j(i)\mathbf{\Phi}_j^{\dagger}(i)}{(1+r_{min}(i))^{2\alpha}}\right)=\sigma_z^2\mathbf{I_M}+\sum_{i\geqslant 1}\frac{PE_{\mathbf{\Phi}}\left(\mathbf{\Phi}_j(i)\mathbf{\Phi}_j^{\dagger}(i)\right)}{(1+r_{min}(i))^{2\alpha}}=\sigma_z^2\mathbf{I_M}+\sum_{i\geqslant 1}\frac{L_iP\cdot\mathbf{I_M}}{(1+r_{min}(i))^{2\alpha}}. \tag{48}$$

Because $\mathbf{\Phi}_j(i)$ is a $M\times L_i$ matrix with iid zero mean unit variance entries, $E_{\mathbf{\Phi}}\left(\mathbf{\Phi}_j(i)\mathbf{\Phi}_j^{\dagger}(i)\right)$ becomes $L_i\cdot\mathbf{I_M}$ in the third line of (48), which completes the proof. □

Finally, the ergodic capacity is derived as $C_j=E_{L_i}\{C_j(\mathbf{\Phi})\}$. Note that the probability distribution of the random variable L_i follows the binomial distribution according to its definition in Section 2.4.

Lemma 8. *The ergodic capacity of a receiver node in the distributed MIMO cooperative scheme for MANETs is lower bounded by*

$$C_j \geqslant \frac{M}{9}\log_2\left[1+\frac{\varphi(M,P,\gamma,\alpha,a_{cell})}{\eta(\sigma_z^2,\mathcal{A},a_{cell},P,\alpha,M,\rho)}\right], \tag{49}$$

where $\eta(\sigma_z^2,\mathcal{A},a_{cell},P,\alpha,M,\rho)=\sigma_z^2+\frac{8P\,\nu(\mathcal{A},\rho,a_{cell})}{(3\sqrt{a_{cell}})^{2\alpha}}c_4$ *in which* $\nu(\mathcal{A},\rho,a_{cell})=e^{-\rho a_{cell}}\left(1-\frac{\Gamma(2,\rho a_{cell})}{\Gamma(2)}\right)+(\mathcal{A}-1)\left(1-\frac{\Gamma(\mathcal{A}+1,\rho a_{cell})}{\Gamma(\mathcal{A}+1)}\right)$ *and* $c_4:=\sum_{k\geqslant 1}\frac{1}{k^{2\alpha-1}}$ *is a constant determined by* α.

Proof. As we already know from above, the final form of the ergodic capacity is

$$C_j=E_{L_i}\{C_j(\mathbf{\Phi})\}\geqslant E_{L_i}\left\{\frac{M}{9}\log_2\left[1+\frac{\varphi(M,P,\gamma,\alpha,a_{cell})}{\left(\sigma_z^2+\sum_{i\geqslant 1}\frac{L_iP}{(1+r_{min}(i))^{2\alpha}}\right)}\right]\right\}\geqslant\frac{M}{9}\log_2\left[1+\frac{\varphi(M,P,\gamma,\alpha,a_{cell})}{\left(\sigma_z^2+\sum_{i\geqslant 1}\frac{E_{L_i}(L_i)P}{(1+r_{min}(i))^{2\alpha}}\right)}\right]. \tag{50}$$

Since we know that $\log_2\left(a+\frac{b}{c+L_i}\right)$ is a convex function of L_i, for a,b and c constants, we have the last line of (50) by using Jensen's inequality.

For $E_{L_i}(L_i)$, we have

$$\begin{aligned}E_{L_i}(L_i)&=e^{-\rho a_{cell}}\left(\sum_{s_i=2}^{\mathcal{A}}\frac{(\rho a_{cell})^{s_i}(s_i-1)}{s_i!}+(\mathcal{A}-1)\sum_{s_i=\mathcal{A}+1}^{\infty}\frac{(\rho a_{cell})^{s_i}}{s_i!}\right)\leqslant e^{-\rho a_{cell}}\left(\sum_{s_i=2}^{\mathcal{A}}\frac{(\rho a_{cell})^{s_i}}{(s_i-1)!}+(\mathcal{A}-1)\sum_{s_i=\mathcal{A}+1}^{\infty}\frac{(\rho a_{cell})^{s_i}}{s_i!}\right)\\&=e^{-\rho a_{cell}}\left(\rho a_{cell}\sum_{s_i=1}^{\mathcal{A}-1}\frac{(\rho a_{cell})^{s_i}}{s_i!}+(\mathcal{A}-1)\sum_{s_i=\mathcal{A}+1}^{\infty}\frac{(\rho a_{cell})^{s_i}}{s_i!}\right)\\&=e^{-\rho a_{cell}}\left\{\rho a_{cell}\left(\sum_{s_i=1}^{\infty}\frac{(\rho a_{cell})^{s_i}}{s_i!}-\sum_{s_i=\mathcal{A}}^{\infty}\frac{(\rho a_{cell})^{s_i}}{s_i!}\right)+(\mathcal{A}-1)\sum_{s_i=\mathcal{A}+1}^{\infty}\frac{(\rho a_{cell})^{s_i}}{s_i!}\right\}.\end{aligned} \tag{51}$$

From (4), $e^{-\rho a_{cell}}\left(\sum_{s_i=\mathcal{A}+1}^{\infty}\frac{(\rho a_{cell})^{s_i}}{s_i!}\right)=1-\frac{\Gamma(\mathcal{A}+1,\rho a_{cell})}{\Gamma(\mathcal{A}+1)}$. Thus, by applying this to the last line of (51), we can conclude that

$$E_{L_i}(L_i)\leqslant\rho a_{cell}\left(\frac{\Gamma(\mathcal{A},\rho a_{cell})}{\Gamma(\mathcal{A})}-\frac{\Gamma(1,\rho a_{cell})}{\Gamma(1)}\right)+(\mathcal{A}-1)\left(1-\frac{\Gamma(\mathcal{A}+1,\rho a_{cell})}{\Gamma(\mathcal{A}+1)}\right):=\nu(\mathcal{A},\rho,a_{cell}). \tag{52}$$

Next we find out the upper bound of $\sum_{i\geqslant 1}\frac{1}{(1+r_{min}(i))^{2\alpha}}$. In this analysis, we simply assume that the minimum distance between the receiver node j in cell 0 and the other interferers in cell i corresponds to the distance between the centers of each cells. Hence, from Fig. 6, the minimum distance between transmitting nodes in the first 8 surrounding cells and the receiver node j is $3\sqrt{a_{cell}}$ and the minimum distance between transmitting nodes in the second 16 surrounding cells and the receiver node j is $2\cdot 3\sqrt{a_{cell}}$. By continuing this step to the entire cells, we can find out the upper bound of $\sum_{i\geqslant 1}\frac{1}{(1+r_{min}(i))^{2\alpha}}$ as follows

$$\sum_{i\geqslant 1}\frac{1}{(1+r_{min}(i))^{2\alpha}}\leqslant\sum_{k\geqslant 1}\frac{8k}{(1+3k\sqrt{a_{cell}})^{2\alpha}}=\frac{8}{(3\sqrt{a_{cell}})^{2\alpha}}\sum_{k\geqslant 1}\frac{k}{\left(k+\frac{1}{3\sqrt{a_{cell}}}\right)^{2\alpha}}\leqslant\frac{8}{(3\sqrt{a_{cell}})^{2\alpha}}\sum_{k\geqslant 1}\frac{1}{k^{2\alpha-1}}=\frac{8}{(3\sqrt{a_{cell}})^{2\alpha}}c_4, \tag{53}$$

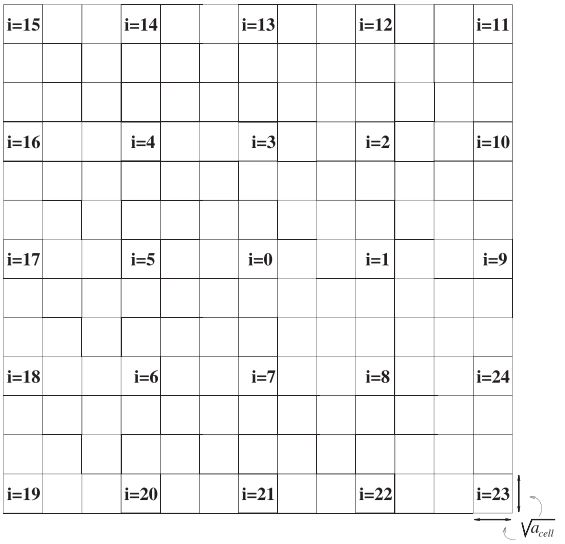

Fig. 6. Cell numbering for simultaneously communication for lower bound computation.

in which $c_4 := \sum_{k\geqslant 1} \frac{1}{k^{2\alpha-1}}$ is a constant determined by α, since we assume that $\alpha \geqslant 2$. Thus, by combining (53) and (52) with (50), and by letting $\eta(\sigma_z^2, \mathcal{A}, a_{cell}, P, \alpha, M, \rho) := \sigma_z^2 + \frac{8P\, v(\mathcal{A},\rho,a_{cell})}{(3\sqrt{a_{cell}})^{2\alpha}} c_4$, we prove the lemma. □

The final result in Lemma 8 shows that the lower bound of the ergodic MIMO capacity also linearly increase with the number of receiving antennas M. Therefore, from (29) and (49), for the distributed MIMO communication scheme proposed in this paper for MANETs, in which during transmissions the nodes send packets from only one of their antennas, while during reception, they use all of their antennas to receive and decode packets from multiple close nodes simultaneously, the ergodic capacity grows linearly with the number of receiving antennas M.

4. Simulation results

The numerical and simulation results presented here were obtained assuming that the maximum number of nodes allowed to communicate in a cell is $\mathcal{A}$ (as said in Section 2.1), and considering the effect from the two hops of interference [34].

Figs. 7 and 8 show the receiver node capacity bounds and the Monte-Carlo simulation results for the capacity of the cooperative MIMO scheme as function of the transmit power P, for two sets of parameters respectively. The resultant upper

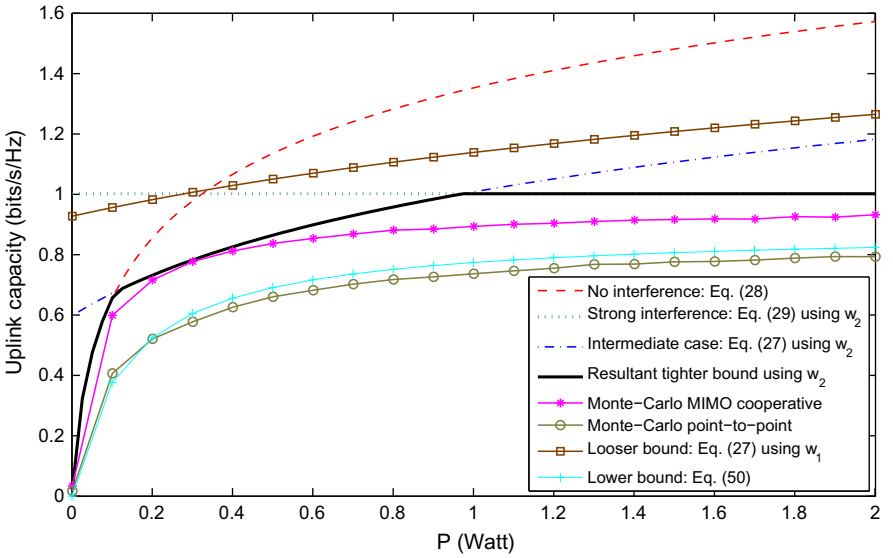

Fig. 7. Uplink capacity as function of power (P) for $M = 2$, $a_{cell} = 2\ \mathrm{m}^2$, $\rho = 3\ \mathrm{nodes/m}^2$, $\sigma_z^2 = 0.01$, $\alpha = 2$, and $\mathcal{A} = 6$.

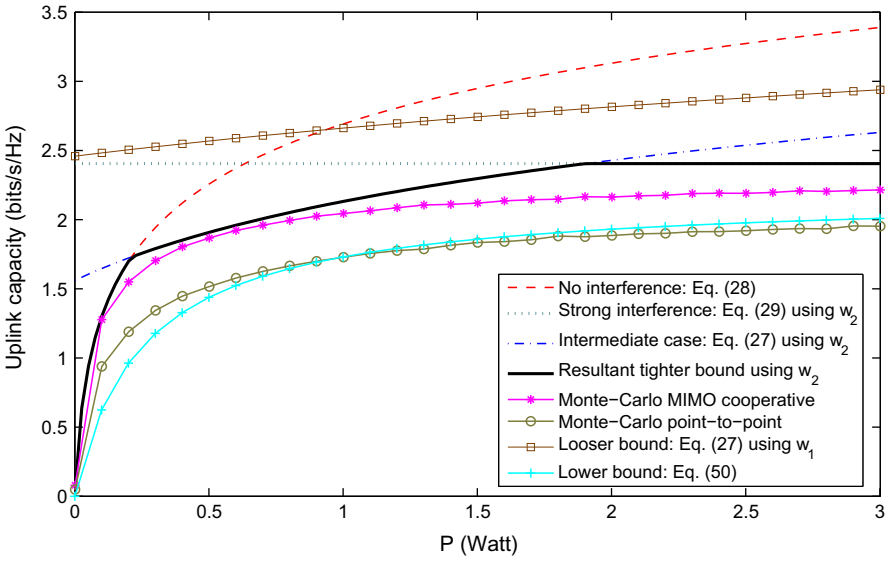

Fig. 8. Uplink capacity as function of power (P) for $M = 4$, $a_{cell} = 4\ \mathrm{m}^2$, $\rho = 2\ \mathrm{nodes/m}^2$, $\sigma_z^2 = 0.01$, $\alpha = 2$, and $\mathcal{A} = 10$.

bound is indicated by the solid line obtained by considering the lower-part curve from the intersection of the three curves given by (27)–(29) where w_2 from (26) was used. The upper bound using w_1 from (24) is also shown, as well as the lower bound from (49). The Monte-Carlo simulations for each curve were obtained by averaging over 15,000 random network topologies. Unlike our analytical model that interfering nodes are assumed to be located in the center of each interfering cell, the nodes are randomly distributed in the simulation area. We observe that the ergodic capacity increases with the increase of the power up to a point where interference is dominant such that practically no increase in capacity is possible by increasing P. The results show that the bounds obtained are close to the simulations.

Our proposed cooperation allows nodes inside a cell to cooperate and no longer compete, by employing a distributed MIMO concept. Also, note that the adjacent interfering cells are in the same symmetric distance for any given cell. Therefore, the Wishart matrices for these channels can be bundled together which makes Lemma 2 a reasonable approach for computation of the upper bound capacity. Figs. 7 and 8 also show that the approach in (24) provides a looser bound because there the Wishart matrices with the same distance from the center cell are considered separately, i.e., multiplied by different coefficients.

In addition, Figs. 7 and 8 present the Monte-Carlo simulations for the MIMO point-to-point communication approach. In this case, we model each node using M antennas for transmission and reception. Each node uses total transmit power P. Also, in the point-to-point technique, only one pair of nodes per cell is able to communicate successfully [21]. We observe that our scheme outperforms the point-to-point case. The cooperative MIMO communication is a framework that allows simultaneous many-to-many communication. Moreover, our approach is a distributed MIMO system that supports more than M transmit antennas (i.e., $\mathcal{A} - 1 > M$). Hence, cooperative MIMO communication increases the average node capacity.

5. Conclusions

The computation of a tight bound on the achievable capacity of MANETs with nodes having multiple antennas is an important and difficult problem. We have introduced a new MIMO cooperative scheme for such networks and computed upper and lower bounds for per node ergodic capacity. Our proposed many-to-many communication approach demonstrates capacity improvement compared to non-cooperative communication schemes. This capacity improvement is achieved at the expense of increase in receiver complexity for each node. The results also demonstrate that the capacity of MIMO mobile ad hoc networks increases linearly with the number of receiving antennas M.

Future work should concentrate on issues like downlink capacity analysis, the effect of channel variations, channel coherence time, memory in the channel, channel estimation, and other practical aspects of mobility on the capacity of the cooperative MIMO communication scheme.

This paper does not discuss the ramifications of this approach at higher layers of the network. It appears that cooperative MIMO communication also provides some advantages at higher layers of the network [38,39].

Acknowledgments

This research was supported in part by CAPES and CNPq/Brazil, by the US Army Research Laboratory under the Network Science Collaborative Technology Alliance, Agreement Number W911NF-09-0053, by Army Research Office under

Agreement Number W911NF-05-1-0246, by the National Science Foundation under Grant CCF-0729230, and by the Baskin Chair of Computer Engineering. The views and conclusions contained in this document are those of the author(s) and should not be interpreted as representing the official policies, either expressed or implied, of the US Army Research Laboratory or the US Government. The US Government is authorized to reproduce and distribute reprints for Government purposes notwithstanding any copyright notation hereon.

References

[1] G.J. Foschini, M.J. Gans, On limits of wireless communications in a fading environment when using multiple antennas, Wireless Personal Communications 6 (1998) 311–355.
[2] E. Telatar, Capacity of multi-antenna Gaussian channels, European Transactions on Telecommunications 10 (6) (1999) 585–595.
[3] A.J. Goldsmith, S.A. Jafar, N. Jindal, S. Vishwanath, Capacity limits of MIMO channels, IEEE Journal on Selected Areas in Communications 21 (5) (2003) 684–702.
[4] A. Jovičić, P. Viswanath, S.R. Kulkarni, Upper bounds to transport capacity of wireless networks, IEEE Transactions on Information Theory 50 (11) (2004) 2555–2565.
[5] G. Luan, J. Gao, A grouped sphere decoding method for virtual MIMO system in clustering ad hoc networks, in: Proc. of International Conference on Wireless Communications, Networking and Mobile Computing (WiCOM), Wuhan, China, September 2011.
[6] B. Chen, M.J. Gans, Limiting throughput of MIMO ad hoc networks, in: Proc. of IEEE International Conference on Acoustics, Speech, and Signal Processing, Philadelphia, PA, USA, March 2005.
[7] R. Blum, MIMO capacity with interference, IEEE Journal on Selected Areas in Communications 21 (5) (2003) 793–801.
[8] S. Aeron, V. Saligrama, Wireless ad hoc networks: strategies and scaling laws for the fixed SNR regime, IEEE Transactions on Information Theory 53 (6) (2007) 2044–2059.
[9] A. Özgür, O. Lévêque, D. Tse, Hierarchical cooperation achieves optimal capacity scaling in ad hoc networks, IEEE Transactions on Information Theory 53 (10) (2007) 3549–3572.
[10] J. Ghaderi, L. Xie, X. Shen, Throughput optimization for hierarchical cooperation in ad hoc networks, in: Proc. of IEEE International Conference on Communications (ICC), Beijing, China, May 2008.
[11] P. Gupta, P.R. Kumar, The capacity of wireless networks, IEEE Transactions on Information Theory 46 (2) (2000) 388–404.
[12] N. Jindal, J.G. Andrews, S. Weber, Multi-antenna communication in ad hoc networks: achieving MIMO gains with SIMO transmission, IEEE Transactions on Communications 59 (2) (2011) 529–540.
[13] V.V. Zaharov, H. Kettani, MIMO ad hoc network performance in the presence of co-channel interference, in: Proc. of International Conference on Computer Research and Development (ICCRD), Kuala Lumpur, Malaysia, May 2010.
[14] T. Elbatt, On the scheduling multiplexing and diversity trade-off in MIMO ad hoc networks: a unified framework, Ad Hoc Networks 11 (2) (2013) 639–653.
[15] Q. Qu, B. Milstein, D.R. Vaman, Cooperative and constrained MIMO communications in wireless ad hoc/sensor networks, IEEE Transactions on Wireless Communications 9 (10) (2010) 3120–3129.
[16] S. Chu, X. Wang, Opportunistic and cooperative spatial multiplexing in MIMO ad hoc networks, IEEE/ACM Transactions on Networking 18 (5) (2010) 1610–1623.
[17] R.M. de Moraes, H.R. Sadjadpour, J.J. Garcia-Luna-Aceves, Many-to-many communication: a new approach for collaboration in MANETs, in: Proc. of IEEE Conference on Computer Communications (Infocom), Anchorage, Alaska, USA, May 2007.
[18] R.M. de Moraes, H.R. Sadjadpour, J.J. Garcia-Luna-Aceves, Many-to-many communication for mobile ad hoc networks, IEEE Transactions on Wireless Communications 8 (5) (2009) 2388–2399.
[19] R.M. de Moraes, H.R. Sadjadpour, J.J. Garcia-Luna-Aceves, Taking full advantage of multiuser diversity in mobile ad hoc networks, IEEE Transactions on Communications 55 (6) (2007) 1202–1211.
[20] A.E. Gamal, J. Mammen, B. Prabhakar, D. Shah, Throughput-delay trade-off in wireless networks, in: Proc. of IEEE Conference on Computer Communications (Infocom), Hong Kong, China, March 2004.
[21] M. Grossglauser, D. Tse, Mobility increases the capacity of wireless ad-hoc networks, in: Proc. of IEEE Conference on Computer Communications (Infocom), Anchorage, Alaska, USA, March 2001.
[22] R. Negi, A. Rajeswaran, Capacity of power constrained ad-hoc networks, in: Proc. of IEEE Conference on Computer Communications (Infocom), Hong Kong, China, March 2004.
[23] S. Toumpis, A.J. Goldsmith, Large wireless networks under fading, mobility, and delay constraints, in: Proc. of IEEE Conference on Computer Communications (Infocom), Hong Kong, China, March 2004.
[24] N. Bansal, Z. Liu, Capacity, delay and mobility in wireless ad-hoc networks, in: Proc. of IEEE Conference on Computer Communications (Infocom), San Francisco, California, USA, March 2003.
[25] B.W. Parkingson, J.J. Spilker, Global Positioning System: Theory and Applications, vol. I, American Institute of Aeronautics and Astronautics, Inc., 1996.
[26] R. Motwani, P. Raghavan, Randomized Algorithms, Cambridge Univ Press, 1995.
[27] F. Baccelli, B. Blaszczyszyn, On a coverage range process ranging from the Boolean model to the Poisson Voronoi tessellation with applications to wireless communications, Advances in Applied Probability 33 (2) (2001) 293–323.
[28] O. Arpacioglu, Z.J. Haas, On the scalability and capacity of single-user-detection based wireless networks with isotropic antennas, IEEE Transactions on Wireless Communications 6 (1) (2007) 8–15.
[29] A.T. James, Distributions of matrix variates and latent roots derived from normal samples, Annals of Mathematical Statistics 35 (2) (1964) 475–501.
[30] C.T. Lau, C. Leung, Capture models for mobile packet radio networks, IEEE Transactions on Communications 40 (5) (1992) 917–925.
[31] F. Zhang, Matrix Theory, Springer-Verlag, 1999.
[32] L.R. Haff, An identity for the Wishart distribution with applications, Journal of Multivariate Analysis 9 (1979) 531–544.
[33] D.V. Rosen, Moments for the inverted Wishart distribution, Scandinavian Journal of Statistics 15 (1988) 97–109.
[34] F. Tobagi, L. Kleinrock, Packet switching in radio channels: Part II – the hidden terminal problem in carrier sense multiple-access and the busy-tone solution, IEEE Transactions on Communications COM-23 (12) (1975) 1417–1433.
[35] A.K. Gupta, D.K. Nagar, Matrix Variate Distributions, Chapman & Hall/CRC, 2000.
[36] R.A. Horn, C.R. Johnsan, Matrix Analysis, Cambridge Press, New York, 1985.
[37] O. Oyman, R.U. Nabar, H. Bolcskei, A.J. Paulraj, Tight lower bound on the ergodic capacity of Rayleigh fading MIMO channels, in: Proc. of IEEE Global Communications Conference (GLOBECOM) 2002, Taipei, Taiwan, China, November 2002.
[38] X. Wang, J.J. Garcia-Luna, H. Sadjadpour, Distributed channel access scheduling for ad hoc networks using virtual MIMO, in: Proc. of IEEE International Conference on Computer Communications (ICCCN), Honolulu, Hawaii, USA, August 2007.
[39] X. Wang, J.J. Garcia-Luna, H. Sadjadpour, Topology aware hybrid channel access using virtual MIMO, in: Proc. of IEEE Symposium on Computers and Communications (ISCC), Aveiro, Portugal, July 2007.